Organometallics **1996,** *15,* 645−654

Syntheses and Structural Characterizations of Metallabis(tricarbadecaboranyl) Sandwiches, $(\eta^4\text{-MeC}_3\text{B}_7\text{H}_9)_2\text{M}$ (M = Ni, Pd, Pt): Tricarbadecaboranyl Analogs of $(\eta^3\text{-C}_3\text{H}_5)_2\text{M}$ Complexes

Beverly A. Barnum, Patrick J. Carroll, and Larry G. Sneddon*

Department of Chemistry, University of Pennsylvania, Philadelphia, Pennsylvania 19104-6323

Received September 25, 1995[⊗]

The reactions of the *nido*-6-Me-5,6,9-$\text{C}_3\text{B}_7\text{H}_9^-$ anion with MX_2 (M = Ni, Pd, Pt) salts yield a series of new bis(tricarbadecaboranyl) $(\eta^4\text{-MeC}_3\text{B}_7\text{H}_9)_2\text{M}$ sandwich complexes including the following: *commo-Pd*-(8-Pd-9-Me-7,9,10-$\text{C}_3\text{B}_7\text{H}_9)_2$ (**1a**), *commo-Pd*-(9-Pd-8-Me-7,8,10-$\text{C}_3\text{B}_7\text{H}_9$)(8′-Pd-9′-Me-7′,9′,10′-$\text{C}_3\text{B}_7\text{H}_9$) (**1b**), *commo-Pd*-(9-Pd-8-Me-7,8,10-$\text{C}_3\text{B}_7\text{H}_9$)(8′-Pd-10′-Me-7′,9′,10′-$\text{C}_3\text{B}_7\text{H}_9$) (**2**), *commo-Pt*-(8-Pt-9-Me-7,9,10-$\text{C}_3\text{B}_7\text{H}_9)_2$ (**3a**), *commo-Pt*-(9-Pt-8-Me-7,8,10-$\text{C}_3\text{B}_7\text{H}_9$)(8′-Pt-9′-Me-7′,9′,10′-$\text{C}_3\text{B}_7\text{H}_9$) (**3b**), and *commo-Ni*-(8-Ni-9-Me-7,9,10-$\text{MeC}_3\text{B}_7\text{H}_9)_2$ (**4a**). X-ray structural determinations and NMR studies of these complexes have revealed that the MC_3B_7 cage fragments in each complex adopt open cage geometries. Previous studies of the coordination properties of the *nido*-6-Me-5,6,9-$\text{C}_3\text{B}_7\text{H}_9^{1-}$ anion demonstrated that it can bind to a transition metal in an η^6-fashion and function as a 5-electron donor ligand similar to an η^5-cyclopentadienyl anion. However, the metal atoms in the $(\eta^4\text{-MeC}_3\text{B}_7\text{H}_9)_2\text{M}$ complexes **1**−**4** are situated in only four-coordinate cage positions, and the structural and spectroscopic data combined with electron-counting arguments suggest that the metals are providing only two orbitals for cluster bonding. Therefore, the $\eta^4\text{-MeC}_3\text{B}_7\text{H}_9^-$ ligands in these complexes appear to function as only bidentate, 3-electron donors to the metal, similar to an $\eta^3\text{-C}_3\text{H}_5^-$ ligand. The $(\eta^4\text{-MeC}_3\text{B}_7\text{H}_9)_2\text{M}$ complexes can thus be considered analogs of $\text{M}(\eta^3\text{-C}_3\text{H}_5)_2$ complexes (M = Ni, Pd, Pt) in which the metals are 16 valence electron systems. The nickel complex **4a** was found to react with PMe_3, but instead of forming an 18 valence electron adduct, oxidation, accompanied by loss of one hydrogen atom, occurred to form the 17 valence electron compound, *commo-Ni*-(1-Ni-5-Me-2,3,5-$\text{C}_3\text{B}_7\text{H}_9$)(9′-Ni-7′-Me-11′-$\text{PMe}_3$-7′,8′,10′-$\text{C}_3\text{B}_7\text{H}_8$) (**5**). An X-ray investigation demonstrated that the PMe_3 is attached to a boron atom on the tricarbadecaboranyl cage that is coordinated to the nickel in an η^4-fashion, while the other tricarbadecaboranyl cage is coordinated to the nickel in a distorted η^6-manner. The distorted cage fragment exhibits a geometry that is intermediate between those found for 11-vertex nido (26 skeletal electrons) and closo (24 skeletal electrons) cage systems, suggesting that the odd electron in **5** may be localized in a cage-centered orbital.

Introduction

Earlier investigations of the transition metal-coordinating properties of the new *nido*-6-Me-5,6,9-$\text{C}_3\text{B}_7\text{H}_9^-$ tricarbadecaboranyl monoanion[1] (Figure 1) demonstrated that it can bind to a transition metal in an η^6-fashion and function as a 5-electron donor ligand similar to an η^5-cyclopentadienyl anion (Figure 2a).[2] A wide variety of metallocene analogs,[2a,b] including tricarbadecaboranyl complexes corresponding to ferrocene and cobaltocene, and hybrid tricarbadecaboranyl triple-decker complexes[2d] have now been characterized and shown to have properties, such as enhanced oxidative and hydrolytic stabilities, that complement their organometallic counterparts. In this paper, we report the syntheses and structural characterizations of a series of new platinum group metallabis(tricarbadecaboranyl) complexes, $(\eta^4\text{-MeC}_3\text{B}_7\text{H}_9)_2\text{M}$ (M = Ni, Pd, Pt), which demonstrate that the tricarbadecaboranyl ligand has variable metal-coordinating and electron-donating properties. In these $(\eta^4\text{-MeC}_3\text{B}_7\text{H}_9)_2\text{M}$ complexes, the tricarbadecaboranyl cages are functioning not as η^6, 5-electron donors, but rather as η^4, 3-electron ligands (Figure 2b). These complexes can therefore be considered as analogs of the known $(\eta^3\text{-C}_3\text{H}_5)_2\text{M}$ compounds (M = Ni, Pd, Pt).[3]

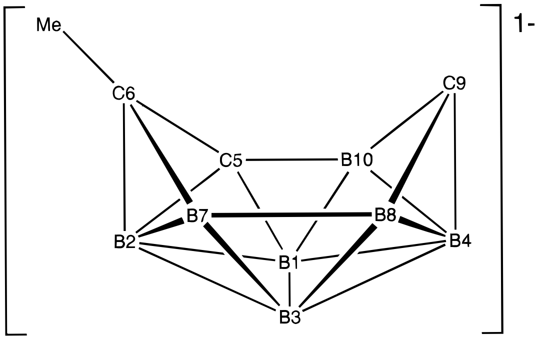

Figure 1. Structure and numbering of the *nido*-6-Me-5,6,9-$\text{C}_3\text{B}_7\text{H}_9^-$ tricarbadecaboranyl anion.

[⊗] Abstract published in *Advance ACS Abstracts,* January 1, 1996.

[1] Kang, S. O.; Furst, G. T.; Sneddon, L. G. *Inorg. Chem.* **1989**, *28*, 2339−2347.

[2] (a) Plumb, C. A.; Carroll, P. J.; Sneddon, L. G. *Organometallics* **1992**, *11*, 1665−1671. (b) Plumb, C. A.; Carroll, P. J.; Sneddon, L. G. *Organometallics* **1992**, *11*, 1672−1680. (c) Plumb, C. A.; Carroll, P. J.; Sneddon, L. G. *Organometallics* **1992**, *11*, 1681−1684. (d) Weinmann, W.; Wolf, A.; Pritzkow, H.; Siebert, W.; Barnum, B. A.; Carroll, P. J.; Sneddon, L. G. *Organometallics* **1995**, *14*, 1911−1919.

0276-7333/96/2315-0645\$12.00/0

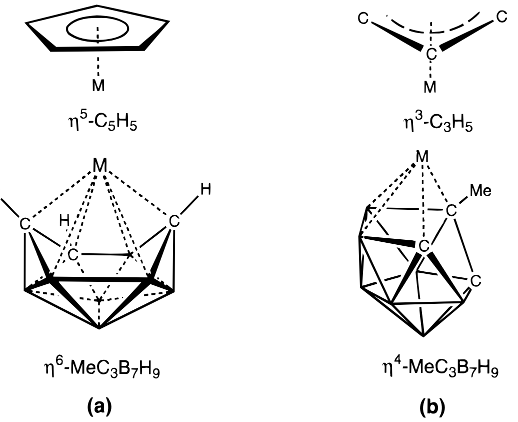

Figure 2. Cyclopentadienyl, $(\eta^5\text{-}C_5H_5)^-$; π-allyl, $(\eta^3\text{-}C_3H_5)^-$; and η^6- and η^4-*nido*-6-Me-5,6,9-$C_3B_7H_9^-$ tricarbadecaboranyl ligands.

Experimental Section

General Procedures and Materials. Unless otherwise noted, all reactions and manipulations were performed in dry glassware under a nitrogen atmosphere using the inert-atmosphere techniques described by Shriver.[4] The $Na^+(6\text{-Me-}5,6,9\text{-}C_3B_7H_9)^-$/THF was prepared as previously reported.[1,2a] The $PtBr_2$, $NiBr_2$ (Strem Chemicals), $PdBr_2$, and $PdCl_2$ (Aldrich) were used as received. Solvents were distilled from appropriate drying agents under nitrogen before use.

^{11}B NMR at 160.5 MHz, ^{13}C NMR at 125.7 MHz, and ^{1}H NMR at 500 MHz were obtained on a Bruker AM 500 spectrometer equipped with the appropriate decoupling accessories. ^{11}B NMR at 64.3 MHz, ^{13}C NMR at 50.3 MHz, and ^{1}H NMR at 200.1 MHz were obtained on a Bruker AC200 spectrometer equipped with the appropriate decoupling accessories. All ^{11}B chemical shifts are referenced to external $BF_3{\cdot}OEt_2$ (0.0 ppm) with a negative sign indicating an upfield shift. Proton and carbon chemical shifts were measured relative to internal residual protons and carbons from the lock solvent and are referenced to TMS (0.0 ppm). NMR data are presented in Table 1. Measurement of the effective magnetic moment for paramagnetic complex **5** was accomplished by the Evans method[5] using a 2 mm coaxial insert.

High- and low-resolution mass spectra were obtained on a VG-ZAB-E high-resolution mass spectrometer. Infrared spectra were obtained on a Perkin-Elmer 1430 spectrophotometer. Preparative thin-layer chromatography was conducted on 0.5 mm (20 × 20 cm) silica gel F-254 plates (Merck 5744). Silica gel (230−400 mesh, Merck) was used for column chromatography. Elemental analyses were obtained from Robertson Microlit Laboratories, Inc. or from the Nesmeyanov Institute of Organoelement Compounds (INEOS), Moscow, Russia.

Palladabis(tricarbadecaboranyl) Complexes: *commo-Pd*-(8-Pd-9-Me-7,9,10-$C_3B_7H_9$)$_2$ (1a), *commo-Pd*-(9-Pd-8-Me-7,8,10-$C_3B_7H_9$)(8′-Pd-9′-Me-7′,9′,10′-$C_3B_7H_9$) (1b), and *commo-Pd*-(9-Pd-8-Me-7,8,10-$C_3B_7H_9$)(8′-Pd-10′-Me-7′,9′,10′-$C_3B_7H_9$) (2). A solution of $Na^+(6\text{-}CH_3\text{-}5,6,9\text{-}C_3B_7H_9)^-$ (3.65 mL of 0.54 M, 1.99 mmol) in THF was added dropwise to a stirring solution of $PdCl_2$ (0.177 g, 1.00 mmol) in THF (15 mL) resulting in a red-rust color. After stirring for 14 h at room temperature, the solvent was vacuum evaporated. The dark residue was dissolved in CH_2Cl_2 and filtered. The solvent was vacuum evaporated, and the red-orange solid (0.275 g, 0.73 mmol, 73% crude yield) was chromatographed two times on TLC plates (silica gel/hexane) to give three bands: **1a**, *commo-Pd*-(8-Pd-9-Me-7,9,10-$C_3B_7H_9$)$_2$, red-orange (R_f 0.51), 0.143 g (38%); **1b**, *commo-Pd*-(9-Pd-8-Me-7,8,10-$C_3B_7H_9$)(8′-Pd-9′-Me-7′,9′,10′-$C_3B_7H_9$), yellow-orange (R_f 0.57), 0.062 g (16%); **2**, *commo-Pd*-(9-Pd-8-Me-7,8,10-$C_3B_7H_9$)(8′-Pd-10′-Me-7′,9′,10′-$C_3B_7H_9$), orange-red (R_f 0.44), 0.015 g (4%). For **1a**: red-orange; mp 140 °C (dec); HRMS calcd for $^{12}C_8{}^1H_{24}{}^{11}B_{14}{}^{106}Pd_1$ 380.2215, found 380.2216; IR (NaCl, CCl_4) 3050 (m), 2990 (m, sh), 2960 (m), 2920 (s), 2855 (m), 2570 (m), 2310 (vw), 2260 (vw), 1715 (vw, br), 1550 (w), 1465 (m), 1425 (w), 1380 (m), 1355 (m, br), 1263 (vs), 1200 (m), 1010 (w, br), 895 (w) cm^{-1}. For **1b**: yellow-orange; mp 137 °C (dec); HRMS calcd for $^{12}C_8{}^1H_{24}{}^{11}B_{14}{}^{106}Pd_1$ 380.2215; found 380.2204; IR (NaCl, CCl_4) 2960 (m), 2925 (m), 2850 (w), 2570 (vs), 1550 (w, br), 1440 (m, br), 1380 (w), 1260 (m), 1190 (m, br), 1145 (w), 1125 (w), 1085 (m), 1055 (w), 1025 (m), 960 (m, br), 920 (w) cm^{-1}. Anal. Calcd for $C_8H_{24}B_{14}Pd$: C, 25.42; H, 6.40. Found: C, 24.84; H, 6.09. For **2**: orange-red, HRMS calcd for $^{12}C_8{}^1H_{24}{}^{11}B_{14}{}^{106}Pd_1$ 380.2215; found 380.2209.

Table 1. NMR Data[a]

cmpd	nucleus	δ (multiplicity, J (Hz), assignment)
1a	^{11}B^{b}	17.9 (d, J = 150, 1B); 11.3 (d, J = 149, 1B); 7.6 (d, J = 143, 1B); −2.2 (d, J = 163, 1B); −4.2 (d, J = 182, 1B); −11.3 (d, J = 160, 2B)
	^{1}H{^{11}B}^{d}	4.81 (s, BH); 3.78 (s, CH); 3.70 (s, CH); 3.29 (s, BH); 2.99 (s, BH); 2.52 (s, BH); 2.15 (s, Me)
1b	^{11}B^{b}	15.9 (d, J = 145, 1B); 15.0 (d, J = 144, 1B); 11.5 (d, J = 148, 1B); 9.3 (d, J = 162, 2B); 7.5 (d, J = 167, 1B); −0.2 (d, J = 151, 1B); −4.5 (d, J = 160, 1B); −8.4 (d, J = 171, 1B); −10.7 (d,^{c} 1B); −12.1 (d,^{c} 1B); −13.4 (d, J = 161, 1B); −14.1 (d,^{c} 1B); −14.9 (d, J = 149, 1B)
	^{1}H{^{11}B}^{d}	5.04 (s, CH); 4.55 (s, BH), 4.31 (s, BH); 4.02 (s, CH); 3.78 (s, CH); 3.60 (s, BH); 3.59 (s, CH); 3.45 (s, BH); 2.70 (s, BH); 2.18 (s, Me); 2.09 (s, Me)
2	^{11}B^{b}	17.4 (d,^{c} 1B) 16.5 (d,^{c} 1B); 14.2 (d,^{c} 1B); 12.4 (d, J = 165, 1B), 8.6 (d,^{c} 1B); 7.2 (d,^{c} 1B); 6.4 (d,^{c} 1B); −1.0 (d, J = 157, 1B); −5.2 (d,^{c} 1B); −7.6 (d,^{c} 1B); −10.2 (d, J = 177, 1B); −12.0 (d,^{c} 1B); −14.9 (d,^{c} 1B); −15.6 (d,^{c} 1B)
3a	^{11}B^{b}	11.1 (d, J = 150, 1B); 3.5 (d,^{c} 2B); −6.2 (d, J = 151, 1B); −7.0 (d, J = 145, 1B); −15.5 (d, J = 164, 1B); −17.2 (d, J = 150, 1B)
	^{1}H^{d}	4.16 (s, br, CH); 3.50 (s, br, CH); 1.98 (s, Me)
3a−b	^{11}B^{b}	13.8 (d, J = 158 Hz, 1B); 13.0 (d, J = 157, 1B); 11.8 (d, J = 154, 1B); 10.3 (d, J = 162, 1B); 5.7 (d, J = 160, 1B); 5.2 (d,^{c} 1B); −3.1 (d, J = 171, 1B); −4.1 (d, J = 170, 1B); −5.3 (d, J = 180, 1B); −7.2 (d,^{c} 1B);−13.4 (d, J = 162, 3B); −15.0 (d, J = 160, 1B)
	^{1}H^{d}	4.12 (s, CH); 4.06 (s, CH); 3.81 (s, CH); 3.52 (s, 2CH); 3.32 (s, br, CH); 1.96 (s, Me); 1.93 (s, Me); 1.36 (s, Me)
4a	^{11}B^{b}	12.6 (d, J = 148, 1B); 4.0 (d,^{c} 2B); −3.4 (d, J = 162, 1B); −9.5 (d, J = 165, 2B); −12.2 (d, J = 146, 1B)
	^{1}H{^{11}B}^{b}	5.27 (s, BH); 3.34 (s, CH); 3.12 (s, CH); 2.39 (s, BH); 1.45 (s, Me)

[a] CD_2Cl_2 solvent. [b] 160.5 MHz. [c] Unable to resolve coupling due to overlapping resonances. [d] 200.1 MHz.

Platinabis(tricarbadecaboranyl) Complexes: *commo-Pt*-(8-Pt-9-Me-7,9,10-$C_3B_7H_9$)$_2$, (3a) and *commo-Pt*-(9-Pt-8-Me-7,8,10-$C_3B_7H_9$)(8′-Pt-9′-Me-7′,9′,10′-$C_3B_7H_9$) (3b). A solution of $Na^+(6\text{-Me-}5,6,9\text{-}C_3B_7H_9)^-$ (7.4 mL of a 0.23 M solution, 1.04 mmol) in THF was added dropwise to a stirring solution of $PtBr_2$ (0.180 g, 0.52 mmol) in THF (15 mL) resulting in a deep brown cloudy solution. After stirring for 14 h at room temperature, the solvent was vacuum evaporated. The brown residue was dissolved in hot hexane and filtered through a 4 cm plug of silica gel. Vacuum evaporation of the solvent gave a 0.37 g (78% crude yield) of a mixture of platinabis(tricarbadecaboranyl) complexes. Repeated TLC on silica gel plates in hexanes gave only two overlapping orange bands ($R_f \sim 0.4$). Collection of only the leading edge of the band gave 0.032 g (7%) of pure **3a**, *commo-Pt*-(8-Pt-9-Me-7,9,10-$C_3B_7H_9$)$_2$. Crystallization from CH_2Cl_2 of the material from the lower portion of the band gave crystals (**3a−b**) that proved to be a mixture of **3a** and *commo-Pt*-(9-Pt-8-Me-7,8,10-$C_3B_7H_9$)-(8′-Pt-9′-Me-7′,9′,10′-$C_3B_7H_9$) (**3b**). For **3a**: red-orange; mp 203 °C; HRMS calcd for $^{12}C_8{}^1H_{24}{}^{11}B_{14}{}^{195}Pt_1$ 469.2829, found 469.2821;

---

(3) (a) Jolly, P. W.; Wilke, G. *The Organic Chemistry of Nickel*; Academic Press: New York, 1974; Vol. 1, Chapter VI, pp 329−401, and references therein. (b) Henc, B.; Jolly, P. W.; Salz, R.; Wilke, G.; Benn, R.; Hoffmann, E. G.; Mynott, R.; Schroth, G.; Seevogel, K.; Sekutowski, J. C.; Krüger, C. *J. Organomet. Chem.* **1980**, *191*, 425, and references therein.

(4) Shriver, D. F.; Drezdzon, M. A. *Manipulation of Air Sensitive Compounds*, 2nd ed.; Wiley: New York, 1986.

(5) (a) Evans, D. F. *J. Chem. Soc.* **1959**, 2003−2005. (b) Carlin, R. L. *J. Chem. Educ.* **1966**, *43*, 521−525. (c) Crawford, T. H.; Swanson, J. *J. Chem. Educ.* **1971**, *48*, 382−386.

IR (NaCl, CCl_4) 3040 (m), 3000 (w), 2960 (m), 2920 (m), 2850 (w), 2560 (vs), 1440 (s), 1385 (m), 1375 (m), 1291 (w, sh), 1265 (m), 1195 (m, br), 1130 (s), 1090 (s), 1045 (m, sh), 1030 (m), 1000 (w), 970 (m), 925 (m), 885 (m), 870 (w), 850 (w) cm^{-1}. Anal. Calcd for $C_8H_{24}B_{14}Pt$: C, 20.59; H, 5.18; B, 32.43. Found: C, 22.10; H, 5.19; B, 28.38. For **3a**−**b**: red-orange; HRMS (Cl^-) calcd for $^{12}C_8{}^1H_{24}{}^{11}B_{14}{}^{195}Pt_1$ 469.2829, found 469.2801. Anal. Calcd for $C_8H_{24}B_{14}Pt$: C, 20.59; H, 5.18. Found: C, 18.86; H, 4.98.

Nickelabis(tricarbadecaboranyl) Complexes: *commo-Ni*-(8-Ni-9-Me-7,9,10-$C_3B_7H_9$)$_2$ (4a). A solution of Na^+(6-Me-5,6,9-$C_3B_7H_9$)$^-$ (4.20 mL of a 0.546 M solution, 2.29 mmol) in THF was added dropwise to a yellow suspension of $NiBr_2$ (0.224 g, 1.02 mmol) in glyme (20 mL). The reaction was stirred for 72 h at room temperature, resulting in a deep brown color, and then the solvent was vacuum evaporated. The dark residue was dissolved in CH_2Cl_2 and filtered through a 3 cm plug of silica gel. The solvent was vacuum evaporated to a deep green solid. Overall the yield for **4a**−**b** was 0.29 g (0.87 mmol, 85%). Development on silica gel plates in hexanes yielded only one broad deep green band. Collection of the leading edge gave *commo-Ni*-(8-Ni-9-Me-7,9,10-$C_3B_7H_9$)$_2$ (**4a**). Collection of the lower portion gave only a mixture of **4a** and another compound that exhibited peaks in its ^{11}B NMR spectrum with chemical shifts similar to **1b**, suggesting that it may be **4b**, *commo-Ni*-(9-Ni-8-Me-7,8,10-$C_3B_7H_9$)(8′-Ni-9′-Me-7′,9′,10′-$C_3B_7H_9$). It was not possible to obtain a pure sample of **4b**. For **4a**: green; mp 165 °C; HRMS calcd for $^{12}C_8{}^1H_{24}{}^{11}B_{14}{}^{58}Ni_1$ 332.2534, found 332.2557; IR (NaCl, CCl_4) 2960 (m), 2920 (m), 2855 (m), 2560 (vs), 1550 (vw, br), 1450 (m), 1385 (w), 1260 (s), 1195 (w), 1130 (m, sh), 1095 (s, sh), 1085 (s), 1015 (s), 965 (m), 925 (m), 915 (w), 865 (w) cm^{-1}. Anal. Calcd for $C_8H_{24}B_{14}Ni$: C, 29.09; H, 7.32. Found: C, 27.50; H, 7.15.

***commo-Ni*-(1-Ni-5-Me-2,3,5-$C_3B_7H_9$)(9′-Ni-7′-Me-11′-PMe_3-7′,8′,10′-$C_3B_7H_8$) (5).** A solution of **4a**−**b**, *commo-Ni*-($MeC_3B_7H_9$)$_2$ (0.096 g, 0.29 mmol), in pentane (20 mL) was maintained at −78 °C, while neat PMe_3 (0.03 mL, 0.29 mmol) was added dropwise, resulting in a color change to brown-green. After stirring for 15 h at room temperature, the solution was filtered. The solvent was vacuum evaporated and the dark residue was chromatographed (silica gel/1:3 hexane−CH_2Cl_2) to give 0.012 g (0.03 mmol, 10%) of **5**, *commo-Ni*-(1-Ni-5-Me-2,3,5-$C_3B_7H_9$)(9′-Ni-7′-Me-11′-PMe_3-7′,8′,10′-$C_3B_7H_8$) (R_f 0.62): green, mp 198 °C; paramagnetic ($\mu = 1.58$); HRMS calcd for $^{12}C_{11}{}^1H_{32}{}^{11}B_{14}{}^{31}P_1{}^{58}Ni_1$ 407.2898, found 407.2923; IR (NaCl, CCl_4) 3065 (w), 2950 (vs), 2920 (vs), 2870 (s), 2855 (s), 2545 (m), 1730 (vvs), 1600 (m), 1580 (m), 1505 (vw), 1487 (w), 1460 (s), 1415 (vw), 1377 (m), 1335 (w), 1260 (vvs, br), 1115 (vs, br), 1067 (vs, br), 1035 (s), 1012 (s), 958 (m), 860 (m) cm^{-1}. Anal. Calcd for $C_{11}H_{32}B_{14}PNi$: C, 32.59; H, 7.96. Found: C, 35.00; H, 7.93.

Reaction of *commo-Pt*-($MeC_3B_7H_9$)$_2$ with PMe_3. A solution of **3a**−**b**, *commo-Pt*-($MeC_3B_7H_9$)$_2$ (0.138 g, 0.30 mmol), in pentane (25 mL) was maintained at −78 °C, while neat PMe_3 (0.03 mL, 0.29 mmol) was added dropwise, resulting in a cloudy, orange solution. No evidence of reaction was observed by ^{11}B NMR during the reaction. After stirring for 15 h at room temperature, the solution was filtered and concentrated in vacuo, but no product was isolated.

Crystallographic Data for 1b, 2, 3a, 3a−b, and 5. Single crystals were grown by slow evaporation in air of methylene chloride solutions.

Collection and Reduction of the Data. X-ray intensity data for **2**, **3a**, and **3a**−**b** were collected on an Enraf-Nonius CAD4 diffractometer employing graphite-monochromated Mo Kα radiation ($\lambda = 0.710\,73$ Å) and using the ω-2θ scan technique. The intensity data were corrected for Lorentz and polarization effects, and an empirical absorption correction was applied. X-ray intensity data for **1b** were collected on an Raxis diffractometer employing graphite-monochromated Mo Kα radiation ($\lambda = 0.710\,73$ Å). X-ray intensity data for **5** were collected on an MSC/R-AXIS IIc area detector employing graphite-monochromated Mo Kα radiation ($\lambda = 0.710\,73$ Å). The intensity data were corrected for Lorentz and polarizations effects but not for absorption.

Solution and Refinement of the Structures. X-ray data for **2**, **3a**, and **3a**−**b** were processed, and the structures were solved and refined using the Enraf-Nonius MolEN[6] structure package on a DEC MicroVAX 3100 computer. The structures for **2**, **3a**, and **3a**−**b** were solved by standard heavy-atom Patterson techniques followed by weighted Fourier syntheses. Refinement was by full-matrix least-squares techniques based on F to minimize the function $\sum w(|F_o| - |F_c|)^2$ with $w = 1/\sigma^2(F)$. Non-hydrogen atoms were refined anisotropically, and hydrogen atoms were included as constant contributions to the structure factors and not refined. For **3a**, non-hydrogen atoms were refined anisotropically; hydrogen atoms could not be located due to the disorder of the two carbaborane cages.[7] X-ray data for **1b** and **5** were processed, and the structure was solved and refined using the Molecular Structure Corp. teXsan[8] package on a Silicon Graphics Indigo R4000 computer. The structures were solved by direct methods (SAP191[9] and SIR88,[10] respectively). Refinement was by full-matrix least-squares techniques based on F to minimize the quantity $\sum w(|F_o| - |F_c|)^2$ with $w = 1/\sigma^2(F)$. For **1b**, non-hydrogen atoms were refined anisotropically, and hydrogen atoms were refined isotropically. For **5**, non-hydrogen atoms were refined anisotropically, cage hydrogens were refined isotropically, and all other hydrogen atoms were included as constant contributions to the structure factors and were not refined.

Crystal and refinement data are given in Table 2. Refined positional parameters are given in Tables 3−7. Selected intramolecular bond distances are presented in Table 8.

Results

The reactions of 2 equiv of the *nido*-6-Me-5,6,9-$C_3B_7H_9^-$ anion with the metal dihalides, M = Pd, Pt, Ni, were found to produce metallabis(tricarbadecaboranyl) products **1**−**4** in good overall yields (>70%). That several isomeric products are produced in each reaction comes about for two reasons. First, as shown in eq 1,

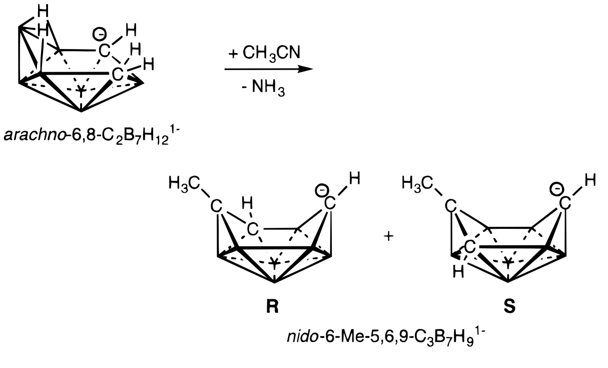

(1)

the 6-Me-5,6,9-$C_3B_7H_9^-$ anion is synthesized as a racemic mixture.[11] Thus, as shown in Figure 3, when a biscage complex is formed, two types of isomeric complexes

---

[6] MolEN, An Interactive Structure Solution Procedure, Enraf-Nonius, Delft, The Netherlands, 1990.

[7] For **3a**: The Pt atom was found to lie on a crystallographic twofold axis which caused the carbaborane cages to be rotationally disordered. The cage atoms were refined with multiplicities of 0.50.

[8] teXsan: Crystal Structure Analysis Package, Molecular Structure Corp., 1985 and 1992.

[9] Fan, H.-F. *R-SAPI88: Structure Analysis Programs with Intelligent Control*; Rigaku Corp., Tokyo, Japan, 1988.

[10] Burla, M. C.; Camalli, M.; Cascarano, G.; Giacovazzo, C.; Polidori, G.; Spagna, R.; Viterbo, D. *J. Appl. Crystallogr.* **1989**, *72*, 389−393.

[11] A modification of the *R* and *S* notation for configuration specification is utilized here. Observation of the carbaborane cage from the open face is thus prioritized from the methylated carbon, where the configuration is specified *R*, for a clockwise direction, or *S* for the counterclockwise configuration.

Table 2. Crystallographic Data Collection and Structure Refinement Information

	1b	**2**	**3a**	**3a−b**	**6**	**7**	**5**
formula	$C_8H_{24}B_{14}Pd$	$C_8H_{24}B_{14}Pd$	$C_8H_{24}B_{14}Pt$	$C_8H_{24}B_{14}Pt$	$C_9H_{17}B_7Ni$	$C_9H_{17}B_7Co$	$C_{11}H_{32}B_{14}NiP$
fw	378.03	378.03	466.72	466.72	259.60	259.84	394.30
space group	$P\bar{1}$	$C2/c$	$C2/c$	$P2_1/c$	$P2_1$	$I2/a$ (No. 15)	$P2_1/n$
Z	1	8	4	6	2	8	4
cell constants							
a (Å)	7.8153(8)	27.771(7)	6.554(3)	17.898(3)	8.6982(4)	14.4637(7)	7.9746(3)
b (Å)	8.8363(7)	8.093(2)	20.590(3)	10.948(1)	10.0330(5)	7.9481(7)	20.7497(8)
c (Å)	6.9753(8)	19.952(3)	13.349(3)	14.127(2)	8.0877(3)	22.689(2)	13.6995(6)
α (deg)	97.682(7)						
β (deg)	113.504(5)	128.26(2)	103.48(3)	108.12(3)	117.017(2)	94.027(4)	100.910(2)
γ (deg)	80.843(7)						
V (Å^3)	434.79(8)	3521(3)	1752(2)	2631(2)	628.78(5)	2601.9(3)	2225.9(1)
μ (cm^{-1})	10.49	10.23	80.76	80.66	15.05	12.83	9.37
cryst size (mm)	0.38 × 0.17 × 0.20	0.20 × 0.20 × 0.40	0.75 × 0.10 × 0.375	0.35 × 0.15 × 0.18	0.22 × 0.22 × 0.10	0.36 × 0.12 × 0.01	0.45 × 0.07 × 0.003
D_{calcd} (g/cm^3)	1.444	1.426	1.770	1.767	1.371	1.327	1.177
radiation (λ, Å)	Mo Kα, 0.710 73	Mo Kα, 0.710 73	Mo Kα, 0.710 73	Mo Kα, 0.710 73	Mo Kα, 0.710 73	Mo Kα, 0.710 73	Mo Kα, 0.710 73
θ range (deg)	2.0−27.0	2.0−27.5	2.0−27.5	2.0−27.5	2.0−25.0	2.0−25.0	2.0−25.0
h,k,l collected	±9,±11,±8	+36,+10,±25	±8,±26,±17	±23,+14,+18	±10,±11,±9	±16,±19,±26	±9,±24,±16
no. of rflns measd	4692	4404	2741	6600	6075	11429	16870
no. of unique rflns	4692	4027	2011	6030	1083[b]	3237[c]	3862
no. of obsd rflns	1719[a]	3606[a]	1838[a]	4554[a]	1637[a]	1047[a]	2823[a]
no. of params	155	208	204	313	154	154	312
R_1	0.031	0.054	0.037	0.033	0.030	0.046	0.053
R_2	0.038	0.072	0.054	0.040	0.042	0.061	0.063

[a] $F^2 > 3.0\sigma$. [b] $R_{merge} = 5.34$. [c] $R_{merge} = 5.04$.

Table 3. Refined Positional Parameters for *commo-Pd*-(9-Pd-8-CH_3-7,8,10-$C_3B_7H_9$)-(8′-Pd-9′-CH_3-7′,9′,10′-$C_3B_7H_9$) (1b)

atom	x	y	z	B_{eq}[a] (Å^2)
Pd9	1.0000	0.0000	1.0000	2.63(2)
C7	1.0572(5)	−0.2190(4)	0.6561(5)	3.5(1)
C8	0.9255(4)	−0.2008(3)	0.7654(5)	3.1(1)
C10	1.2776(4)	−0.0597(4)	1.0098(6)	3.3(1)
C12	0.7186(5)	−0.1985(5)	0.6248(7)	4.2(1)
B1	1.2499(6)	−0.3618(4)	1.0155(7)	3.9(1)
B2	1.2626(6)	−0.3299(5)	0.7684(7)	4.2(2)
B3	1.0576(6)	−0.3753(4)	0.7787(7)	3.9(1)
B4	1.0239(5)	−0.2614(4)	0.9963(6)	3.1(1)
B5	1.2589(5)	−0.1780(4)	1.1536(6)	3.4(1)
B6	1.3963(5)	−0.2355(5)	1.0015(7)	3.9(1)
B11	1.2493(6)	−0.1231(5)	0.7806(7)	3.8(1)

[a] $B_{eq} = {}^8/_3[U_{11}(aa^*)^2 + U_{22}(bb^*)^2 + U_{33}(cc^*)^2 + 2U_{12}aabb \cos \gamma + 2U_{13}aacc \cos \beta + 2U_{23}bbcc^* \cos \alpha]$.

Table 4. Refined Positional Parameters for *commo-Pd*-(9-Pd-8-CH_3-7,8,10-$C_3B_7H_9$)-(8′-Pd-10′-CH_3-7′,9′,10′-$C_3B_7H_9$) (2)

atom	x	y	z	B_{eq}[a] (Å^2)
Pd9	0.11611(1)	0.26745(5)	0.10413(2)	2.299(7)
C7	0.0818(2)	0.3724(8)	0.2124(3)	3.2(1)
C8	0.1334(2)	0.4118(8)	0.2111(3)	2.9(1)
C8m	0.1459(3)	0.5936(9)	0.2089(4)	4.2(2)
C10	0.0710(2)	0.0909(8)	0.1261(3)	3.3(1)
B1	0.1618(3)	0.120(1)	0.2975(4)	3.6(2)
B2	0.0930(2)	0.212(1)	0.2745(4)	3.9(1)
B3	0.1530(3)	0.333(1)	0.3040(4)	3.7(2)
B4	0.1814(2)	0.262(1)	0.2476(3)	3.1(1)
B5	0.1422(3)	0.0528(9)	0.1992(3)	3.1(1)
B6	0.0894(3)	0.030(1)	0.2209(4)	3.6(1)
B11	0.0397(3)	0.202(1)	0.1533(4)	3.2(1)
C7′	0.1708(2)	0.4136(8)	0.0857(3)	3.1(1)
C9′	0.0935(2)	0.1227(8)	−0.0017(3)	2.9(1)
C10′	0.1469(2)	0.1208(8)	−0.0012(3)	3.2(1)
C10m′	0.1744(3)	−0.045(1)	0.0049(4)	4.9(2)
B1′	0.0814(3)	0.400(1)	−0.0862(4)	4.0(2)
B2′	0.1569(3)	0.463(1)	−0.0070(4)	3.9(2)
B3′	0.1018(3)	0.4773(9)	0.0115(4)	3.4(1)
B4′	0.0515(3)	0.285(1)	−0.0446(4)	3.4(2)
B5′	0.0780(3)	0.185(1)	−0.0948(4)	3.7(2)
B6′	0.1438(3)	0.274(1)	−0.0612(3)	4.3(1)
B11′	0.1964(3)	0.280(1)	0.0579(4)	3.4(2)

[a] $B_{eq} = {}^4/_3[\beta_{11}a^2 + \beta_{22}b^2 + \beta_{33}c^2 + \beta_{12}ab \cos \gamma + \beta_{13}ac \cos \beta + \beta_{23}bc \cos \alpha]$.

can result: (1) complexes containing two cages of the same enantiomeric type, $S{-}M{-}S$ or $R{-}M{-}R$ (**1a**, **3a**, **4a**) or (2) complexes containing two different enantiomeric forms of the anion, $R{-}M{-}S$ (**1b**, **3b**). Second, as previously demonstrated,[2a−c] cage rearrangements involving the migration of cage carbons can readily occur in these systems to produce additional geometric isomers (**2**).

Palladabis(tricarbadecaboranyl) Complexes 1a, 1b, and 2. The reaction of palladium dihalide with 2 equiv of $Na^+(6\text{-Me-}5,6,9\text{-}C_3B_7H_9)^-$ yielded three isomeric metallabis(tricarbadecaboranyl) products. The compositions of the major products, **1a** and **1b**, were established by elemental analyses and/or exact mass determinations. Smaller amounts of **2** were obtained; therefore, although its structure was established crystallographically, collection of complete spectroscopic and analytical data for this compound was not possible.

$$
\begin{aligned}
&2\textit{nido}\text{-6-Me-5,6,9-}C_3B_7H_9{}^-Na^+ + PdBr_2 \rightarrow 2NaBr + \\
&\quad \textit{commo-Pd}\text{-(8-Pd-9-Me-7,9,10-}C_3B_7H_9)_2\ (\mathbf{1a}) + \\
&\quad \textit{commo-Pd}\text{-(9-Pd-8-Me-7,8,10-}C_3B_7H_9) \\
&\quad (8'\text{-Pd-9}'\text{-Me-7}',9',10'\text{-}C_3B_7H_9)\ (\mathbf{1b}) + \\
&\quad \textit{commo-Pd}\text{-(9-Pd-8-Me-7,8,10-}C_3B_7H_9) \\
&\quad (8'\text{-Pd-10}'\text{-Me-7}',9',10'\text{-}C_3B_7H_9)\ (\mathbf{2}) \qquad (2)
\end{aligned}
$$

After evaporation of solvent, the crude reaction products were separated by chromatography on silica gel plates and the compounds were then recrystallized from CH_2Cl_2. Single-crystal X-ray studies of **1b** and **2** (Figures 4 and 5) demonstrated that the cage fragments in these complexes exhibit similar open cage geometries. Thus, the palladium atom occupies a four-coordinate cage position with normal bond distances from the palladium atom to C10(7′), C8(9′), B4(4′), and B5(3′) in the range of ~2.1−2.3 Å, but greatly increased distances in both compounds from the palladium atom to C7(10′) and B11(11′) of ~2.9−3.0 Å (Table 8). This has the affect of forming an open five-membered ring composed of the Pd9−C8−C7−B11−C10 or Pd8′−C7′−B11′−C10′−C9′ atoms. The C8−C7−B11−C10 (and C7′−B11′−C10′−C9′) atoms form a plane, with the palladium atom distorted out of this plane above the open face (0.87 Å, **1b**; 0.90 and 0.93 Å, **2**).

1a and **1b** differ because they have different enantiomeric compositions. **1b** contains both one R and one S cage enantiomer ($R{-}M{-}S$, Figure 3). As evidenced

Table 5. Refined Positional Parameters for *commo-Pt*-(8-Pt-9-CH_3-7,9,10-$C_3B_7H_9$)$_2$ (3a)

atom	x	y	z	$B_{eq}{}^a$ (Å^2)
Pt8	0.0000	0.15610(2)	0.2500	2.276(6)
C7	0.062(2)	0.1065(8)	0.389(1)	3.4(3)
C9	−0.118(3)	0.0613(9)	0.174(2)	4.0(4)
C9m	−0.264(3)	0.0667(9)	0.069(2)	4.6(4)
C10	−0.189(3)	0.0233(8)	0.255(2)	4.0(4)
B1	0.227(3)	0.005(1)	0.301(2)	4.5(4)
B2	0.160(3)	0.032(1)	0.416(2)	4.0(4)
B3	0.258(3)	0.0874(9)	0.338(2)	3.8(4)
B4	0.134(3)	0.0638(8)	0.195(2)	3.4(4)
B5	−0.019(3)	0.0030(9)	0.193(2)	10.5(4)
B6	−0.011(4)	−0.0174(8)	0.322(3)	6.0(7)
B11	−0.116(4)	0.056(1)	0.379(2)	4.6(4)
C7′	−0.012(3)	0.2396(7)	0.338(1)	3.3(3)
C9′	0.055(2)	0.2196(8)	0.130(1)	2.9(3)
C9m′	0.166(3)	0.187(1)	0.054(1)	4.1(4)
C10′	0.165(3)	0.2796(8)	0.183(1)	3.7(3)
B1′	−0.260(3)	0.3022(9)	0.162(2)	3.9(4)
B2′	−0.120(4)	0.3155(9)	0.301(2)	4.2(4)
B3′	−0.252(3)	0.2391(8)	0.255(1)	3.1(3)
B4′	−0.195(3)	0.221(1)	0.125(1)	3.4(3)
B5′	−0.067(3)	0.2926(8)	0.090(1)	3.1(3)
B6′	0.005(4)	0.3416(8)	0.208(2)	4.1(4)
B11′	0.161(4)	0.288(1)	0.309(1)	4.0(4)

[a] $B_{eq} = {}^4/_3[\beta_{11}a^2 + \beta_{22}b^2 + \beta_{33}c^2 + \beta_{12}ab \cos \gamma + \beta_{13}ac \cos \beta + \beta_{23}bc \cos \alpha]$.

Table 6. Refined Positional Parameters for *commo-Pt*-(8-Pt-9-CH_3-7,9,10-$C_3B_7H_9$)$_2$ + *commo-Pt*-(9-Pt-8-CH_3-7,8,10-$C_3B_7H_9$)-(8′-Pt-9′-CH_3-7′,9′,10′-$C_3B_7H_9$) (3a−b)

atom	x	y	z	$B_{eq}{}^a$ (Å^2)
Pt8	0.83224(1)	0.11750(2)	0.84677(2)	2.487(4)
C7	0.7955(4)	0.0222(7)	0.9533(5)	4.0(2)
C9	0.8011(4)	−0.0439(7)	0.7484(5)	3.9(2)
C9m	0.7889(6)	−0.0258(9)	0.6382(6)	5.8(2)
C10	0.7336(4)	−0.1023(7)	0.7743(7)	4.9(2)
B1	0.8639(6)	−0.1864(9)	0.9166(7)	4.9(2)
B2	0.8003(6)	−0.1283(8)	0.9780(7)	5.0(2)
B3	0.8795(5)	−0.0347(8)	0.9662(6)	3.9(2)
B4	0.8846(5)	−0.0730(8)	0.8375(6)	3.7(2)
B5	0.8158(6)	−0.1918(8)	0.7892(8)	5.3(2)
B6	0.7578(6)	−0.2041(9)	0.8676(9)	5.6(3)
B11	0.7221(5)	−0.0516(9)	0.8821(7)	4.5(2)
C7′	0.8172(4)	0.2789(6)	0.9221(5)	3.3(1)
C9′	0.9107(3)	0.2240(7)	0.7886(4)	3.3(1)
C9m′	0.9704(4)	0.1536(8)	0.7553(6)	4.8(2)
C10′	0.9447(4)	0.3262(8)	0.8595(5)	3.9(2)
B1′	0.8002(5)	0.4089(9)	0.7530(6)	4.2(2)
B2′	0.8068(5)	0.4229(8)	0.8823(7)	4.2(2)
B3′	0.7605(4)	0.2950(7)	0.8096(6)	3.4(2)
B4′	0.8196(4)	0.2546(8)	0.7241(5)	3.3(2)
B5′	0.8925(5)	0.3730(8)	0.7435(7)	4.2(2)
B6′	0.8927(5)	0.4551(9)	0.8466(7)	4.7(2)
B11′	0.8986(5)	0.3453(8)	0.9472(6)	4.0(2)
Pt9″	0.500	0.500	0.500	2.258(6)
C7″	0.4465(4)	0.6915(7)	0.6179(5)	3.5(1)
C8″	0.5172(4)	0.6157(6)	0.6341(4)	3.0(1)
C8m″	0.5462(5)	0.5504(7)	0.7332(5)	4.4(2)
C10″	0.4215(4)	0.6395(6)	0.4212(5)	3.2(1)
B1″	0.5322(5)	0.8113(8)	0.5179(6)	3.7(2)
B2″	0.4446(5)	0.8236(7)	0.5555(6)	3.8(2)
B3″	0.5322(5)	0.7691(7)	0.6370(6)	3.6(2)
B4″	0.5740(4)	0.6643(8)	0.5693(6)	3.2(2)
B5″	0.5111(4)	0.6863(7)	0.4328(5)	3.1(1)
B6″	0.4363(5)	0.7931(7)	0.4342(7)	4.1(2)
B11″	0.3856(5)	0.6968(8)	0.4986(6)	3.7(2)

[a] $B_{eq} = {}^4/_3[\beta_{11}a^2 + \beta_{22}b^2 + \beta_{33}c^2 + \beta_{12}ab \cos \gamma + \beta_{13}ac \cos \beta + \beta_{23}bc \cos \alpha]$.

Table 7. Refined Positional Parameters for *commo-Ni*-(1-Ni-5-Me-2,3,5-$C_3B_7H_9$)(9′-Ni-7′-Me-11′-PMe_3-7′,8′,10′-$C_3B_7H_8$) (5)

atom	x	y	z	$B_{eq}{}^a$ (Å^2)
Ni1	0.04374(7)	0.12133(3)	0.16530(4)	2.78(1)
P13′	0.0260(2)	0.33552(6)	0.12791(10)	3.28(3)
C2	−0.0254(6)	0.0261(2)	0.1766(4)	3.3(1)
C3	−0.0290(6)	0.1530(2)	0.2897(3)	3.3(1)
C5	−0.1830(6)	0.0368(2)	0.2172(4)	3.6(1)
C7′	0.2683(6)	0.2197(2)	0.1068(4)	3.4(1)
C8′	0.2763(6)	0.1490(2)	0.1272(4)	3.3(1)
C10′	−0.0745(6)	0.1971(2)	0.0827(3)	3.0(1)
C12	−0.3500(7)	0.0103(3)	0.1589(5)	5.5(2)
C12′	0.4185(6)	0.2597(3)	0.1601(5)	4.6(1)
C14′	0.1159(8)	0.3533(3)	0.2547(4)	5.9(2)
C15′	−0.1989(7)	0.3467(3)	0.1168(5)	5.2(1)
C16′	0.0951(8)	0.3971(2)	0.0531(5)	5.4(2)
B1′	0.0989(9)	0.1599(3)	−0.0608(5)	4.4(2)
B2′	0.3036(9)	0.1691(3)	0.0129(5)	4.4(2)
B3′	0.1690(8)	0.1067(3)	0.0419(4)	3.7(1)
B4	0.1416(7)	0.0364(3)	0.2555(4)	3.4(1)
B4′	−0.0577(8)	0.1385(3)	0.0111(5)	3.9(1)
B5′	−0.0405(8)	0.2200(3)	−0.0298(4)	3.8(1)
B6	−0.1955(7)	0.1113(3)	0.2731(5)	3.7(1)
B6′	0.1772(8)	0.2379(3)	−0.0142(5)	4.1(1)
B7	0.1387(7)	0.1142(3)	0.3286(4)	3.5(1)
B8	−0.0267(9)	−0.0133(3)	0.2835(5)	4.0(1)
B9	−0.0405(8)	0.1071(3)	0.3878(4)	3.5(1)
B10	0.0816(8)	0.0387(3)	0.3750(5)	3.9(1)
B11′	0.0697(7)	0.2492(2)	0.0881(4)	2.9(1)
B11	−0.1497(9)	0.0376(3)	0.3432(5)	4.2(1)

[a] $B_{eq} = {}^4/_3[\beta_{11}a^2 + \beta_{22}b^2 + \beta_{33}c^2 + \beta_{12}ab \cos \gamma + \beta_{13}ac \cos \beta + \beta_{23}bc \cos \alpha]$.

Table 8. Selected Intramolecular Distances (Å)

Palladium Complexes

1b		2		
Pd−C8(C9′)	2.227(3)	Pd−C8(*C7′)	2.209(6)	*2.128(7)
Pd−C10(C7′)	2.125(3)	Pd−C10(*C9′)	2.117(7)	*2.141(6)
Pd−B4(B4′)	2.285(3)	Pd−B4(*B3′)	2.249(4)	*2.357(8)
Pd−B5(B3′)	2.329(3)	Pd−B5(*B4′)	2.333(7)	*2.335(6)
Pd−C7(C10′)	3.006(3)	Pd−C7(*C10′)	2.979(8)	*2.963(8)
Pd−B11(B11′)	2.929(4)	PdB11(*B11′)	2.884(9)	*2.893(9)

Platinum Complexes

	3a		3a (3a−b)		3b	
Pt−C7(C7′)	2.069(17)	2.091(15)	2.122(7)	2.098(8)	Pt″−C10″	2.139(6)
Pt−C9(C9′)	2.250(18)	2.165(16)	2.174(7)	2.210(7)	Pt″−C8″	2.220(6)
Pt−B3(B3′)	2.308(18)	2.388(18)	2.299(8)	2.335(8)	Pt″−B5″	2.284(8)
Pt−B4(B4′)	2.287(19)	2.279(18)	2.250(8)	2.307(9)	Pt″−B4″	2.267(8)
Pt−C10(C10′)	3.008(17)	2.979(18)	3.014(8)	2.972(7)	Pt″−C7″	3.013(7)
Pt−B11(B11′)	2.892(24)	2.964(21)	2.932(9)	2.950(10)	Pt″−B11″	2.968(9)

Nickel Complexes

	5	*closo*-(η^3-C_3H_5)Ni-($MeC_3B_7H_9$)[2d]	*nido*-(η^3-C_3H_5)Ni-($MeC_3B_7H_9$)[2d]
Ni−C2	2.066(5)	1.997(3)	
Ni−C3	2.012(5)	1.945(3)	
Ni−B4	2.208(5)	2.188(3)	
Ni−B7	2.227(6)	2.248(3)	
Ni−C5	2.709(5)	2.515(3)	
Ni−B6	2.633(6)	2.397(3)	
Ni−C8′(8)	2.100(5)		2.019(5)
Ni−C10′(10)	2.058(5)		1.991(6)
Ni−B3′(4)	2.142(6)		2.093(6)
Ni−B4′(5)	2.144(6)		2.108(7)
Ni−C7′(7)	2.925(5)		2.880(5)
Ni−B11′(B11)	2.878(6)		2.871(7)

by the similarity of its spectral data with that of the structurally determined **3a** (vide infra), **1a** is proposed to have a structure like **3a** containing two tricarbadecaboranyl cages of the same enantiomeric form (either *R*−*M*−*R* or *S*−*M*−*S*, Figure 3). **2** also contains two different enantiomeric cages, but in addition, the methyl group on one of the cages in **2** is at a position (C10′) different from that expected (C9′) based on its position in the starting 6-Me-5,6,9-$C_3B_7H_9^-$ anion (Figure 1). A similar methyl "migration" was found in the conversion of *commo-Fe*-(1-Fe-2-Me-2,3,5-$C_3B_7H_9$)$_2$ to *commo-Fe*-(1-Fe-5-Me-2,3,5-$C_3B_7H_9$)(1-Fe-4-Me-2,3,4-$C_3B_7H_9$)[2a] and

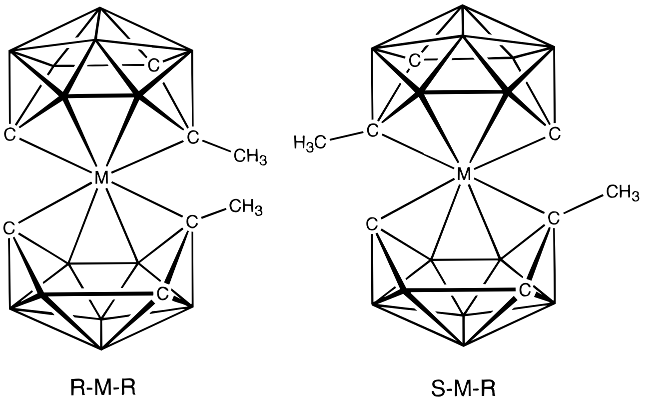

Figure 3. Possible *R*−*M*−*R* and *S*−*M*−*R* structures of $(\eta^4\text{-MeC}_3B_7H_9)_2M$ complexes.

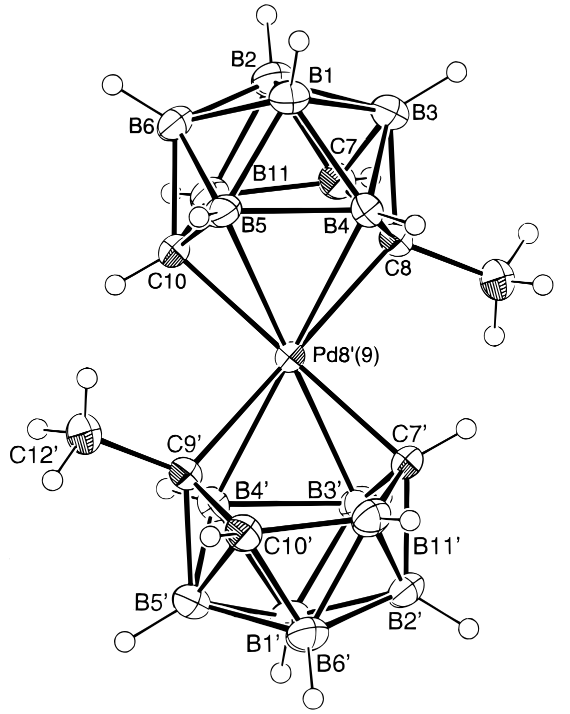

Figure 4. ORTEP drawing of the molecular structure of **1b**, *commo-Pd*-(9-Pd-8-CH_3-7,8,10-$C_3B_7H_9$)(8′-Pd-9′-CH_3-7′,9′,10′-$C_3B_7H_9$).

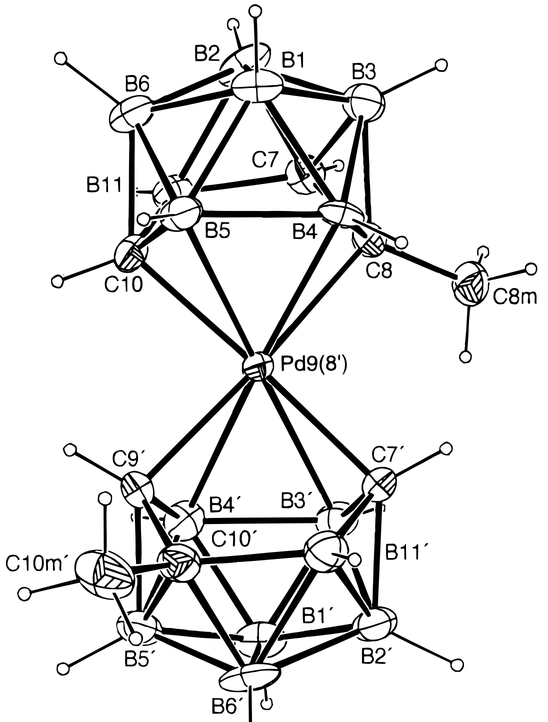

Figure 5. ORTEP drawing of the molecular structure of **2**, *commo-Pd*-(9-Pd-8-CH_3-7,8,10-$C_3B_7H_9$)(8′-Pd-10′-CH_3-7′,9′,10′-$C_3B_7H_9$).

was shown to occur by a mechanism involving a rearrangement of the cage carbon atoms.[2c]

Given the center of symmetry observed in its solid state structure, it is perhaps initially surprising that the ^{11}B NMR spectrum of **1b** exhibits more than seven different resonances, indicating that in solution the two cages are nonequivalent. It should be recognized, however, that in solution the two cages may rotate and since the two cages are different enantiomorphs they are not equivalent. Thus, under these conditions, there are 14 nonequivalent boron atoms, which is consistent with the 13 separate resonances (with one of intensity 2) observed in the 160.5 MHz ^{11}B NMR spectrum. Likewise, the $^{1}H\{^{11}B\}$ NMR spectrum of **1b** clearly shows four C−H and two methyl resonances arising from the two inequivalent cages. On the other hand, the ^{11}B NMR spectrum of **1a** contains only seven resonances and its $^{1}H\{^{11}B\}$ NMR spectrum shows only one methyl and two C−H resonances. The simpler spectra for **1a** arise because in this complex both tricarbadecaboranyl cages are of the same enantiomeric form; therefore, regardless of any rotation, the two cages will be related by a twofold rotation. The equivalent cages then generate only one set of peaks in the ^{11}B and ^{1}H NMR spectra. Because the methyl groups in the two tricarbadecaboranyl cages of **2** are substituted at different positions, the cages are quite different and the ^{11}B NMR spectrum clearly resolves the expected 14 resonances.

Platinabis(tricarbadecaboranyl) Complexes 3a and 3a−b. The reaction of platinum dihalide with 2 equiv of $Na^+(6\text{-Me-}5,6,9\text{-}C_3B_7H_9)^-$ yielded two isomeric metallabis(tricarbadecaboranyl) products.

$$\begin{aligned}2\,nido\text{-6-Me-5,6,9-}C_3B_7H_9{}^-Na^+ + PtBr_2 \rightarrow 2NaBr + \\ commo\text{-}Pt\text{-(8-Pt-9-Me-7,9,10-}C_3B_7H_9)_2\ (\mathbf{3a}) + \\ commo\text{-}Pt\text{-(9-Pt-8-Me-7,8,10-}C_3B_7H_9) \\ (8'\text{-Pt-9'-Me-7',9',10'-}C_3B_7H_9)\ (\mathbf{3b}) \quad (3)\end{aligned}$$

Regardless of the solvent employed as the eluent, only one broad band could be observed by thin-layer chromatography. Separation of **3a** was achieved by repeated TLC chromatography on silica gel plates in hexane in which the leading edge of the band was collected. As shown in Figure 6, the X-ray-determined structure of **3a** established that it is the *S*−Pt−*S*/*R*−Pt−*R* isomer. As in the palladium complexes, the platinum atom sits in a four-coordinate cage position with the bonding distances to the two carbon atoms and two boron atoms in the normal ranges observed in platinacarbaboranes and platinaboranes.[12] Much longer distances are observed between the platinum and the C10(C10′) and B11(B11′) atoms in **3a** (Table 8) giving rise to the open five-membered faces of the cages composed of the Pt8−C7−B11−C10−C9 and Pt8′−C7′−B11′−C10′−C9′ atoms. The platinum atom is distorted above these planes by 0.8−0.9 Å.

Attempts were made to further separate the bottom half of the band from which **3a** was collected in order

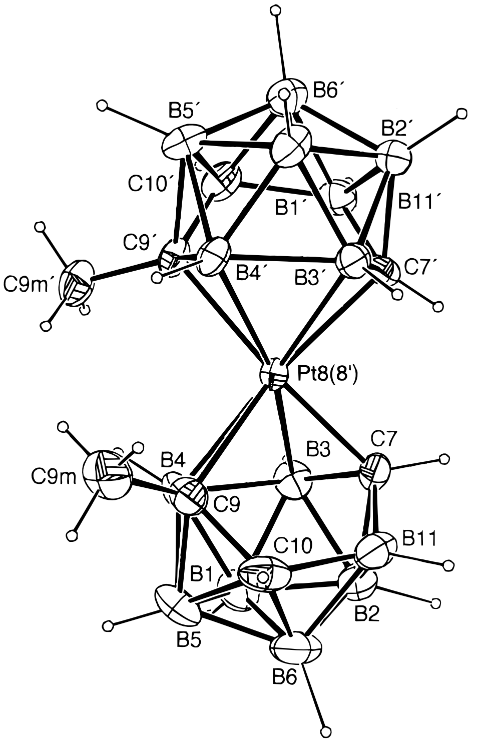

Figure 6. ORTEP drawing of the molecular structure of **3a**, *commo-Pt*-(8-Pt-9-CH$_3$-7,9,10-C$_3$B$_7$H$_9$)$_2$, from **3a**−**b**.

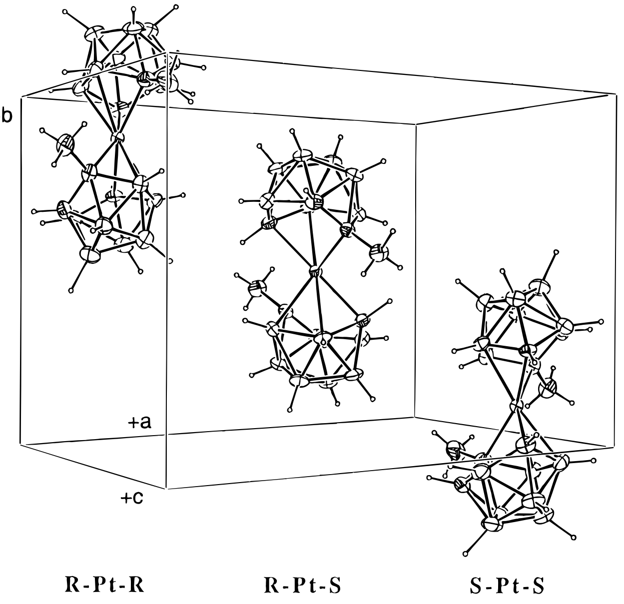

Figure 7. Packing diagram for **3a**−**b**.

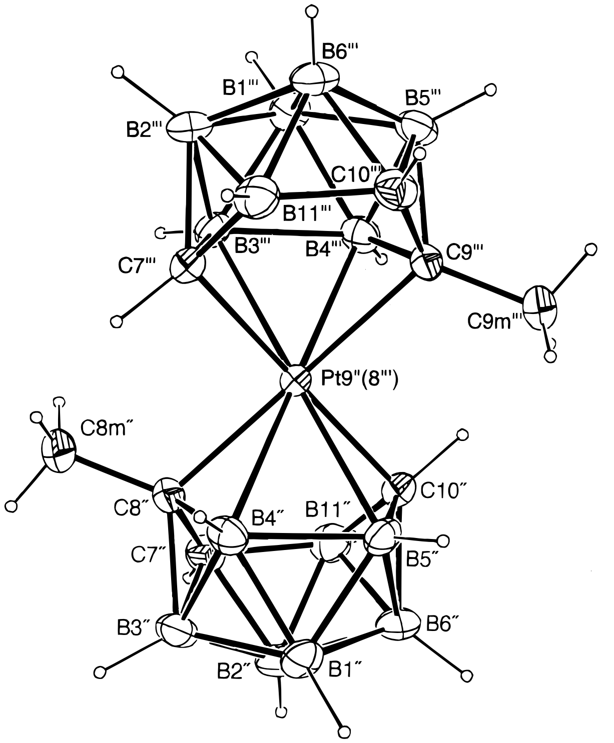

Figure 8. ORTEP drawing of the molecular structure of **3b**, *commo-Pt*-(9-Pt-8-CH$_3$-7,8,10-C$_3$B$_7$H$_9$)(8′-Pt-9′-CH$_3$-7′,9′,10′-C$_3$B$_7$H$_9$), from **3a**−**b**.

to isolate the R−Pt−S isomer. Recrystallization of this material gave, as shown in the packing diagram in Figure 7, what proved to be a co-crystallized mixture of **3a** and **3b**, **3a**−**b**, of the two different platinabis(tricarbadecaboranyl) isomers. Consistent with the crystallographic symmetry dictated by the observed $P2_1/c$ space group with $Z = 6$, the platinum atom of the symmetric R−Pt−S isomer **3b** sits on the crystallographic inversion center, thereby relating the two cages bound to this metal. The platinum atoms of the R−Pt−R and S−Pt−S enantiomers (**3a**) are situated off the inversion center such that these two enantiomeric compounds are related by this center. There are no significant differences in the molecular structures of the R−Pt−R (S−Pt−S) complexes in the **3a** and **3a**−**b** determinations. As can be seen in the ORTEP representation of the molecular structure of **3b**, shown in Figure 8, both of the tricarbadecaboranyl cage fragments exhibit open cage geometries similar to that found for **3a**. Likewise, the bond distances observed in **3b** are again in the normal ranges and are consistent with those found for **3a**.

As expected, the NMR spectra of **3a** are similar to that observed for **1a**, showing only six resonances (one of intensity 2) in its ^{11}B NMR spectrum and only one methyl and two C−H resonances in its ^{1}H NMR spectrum. As discussed above, such spectra are consistent with the R−M−R/S−M−S compositions of **1a** and **3a**. While **3b** could not be separated in pure form, subtraction of those resonances attributed to **3a** from the ^{11}B spectrum obtained for the **3a**−**b** mixture yields a spectrum quite similar to that found for **1b**.

Nickelabis(tricarbadecaboranyl) Complexes 4a. According to its ^{11}B NMR spectrum and initial analytical TLC analysis, the reaction mixture resulting from the reaction of nickel bromide with 2 equiv of Na$^+$(6-Me-5,6,9-C$_3$B$_7$H$_9$)$^-$ appeared to contain, as in the case of the platinum and palladium reactions, a mixture of isomeric products. However, only one metallabis(tricarbadecaboranyl) complex **4a**, could be isolated following workup and preparative chromatographic separation.

$$2\textit{nido}\text{-6-Me-5,6,9-C}_3\text{B}_7\text{H}_9{}^-\text{Na}^+ + \text{NiBr}_2\cdot\text{DME} \rightarrow \\ 2\text{NaBr} + \textit{commo-Ni}\text{-(8-Ni-9-Me-7,9,10-C}_3\text{B}_7\text{H}_9)_2\ (\mathbf{4a}) \tag{4}$$

The composition of **4a** was established by exact mass determinations and elemental analysis. The product could not be obtained in crystalline form, but its ^{11}B NMR spectrum is similar to those observed for **1a** and **3a**, being composed of only six resonances (with one of intensity 2) in similar chemical shift ranges. The ^{1}H

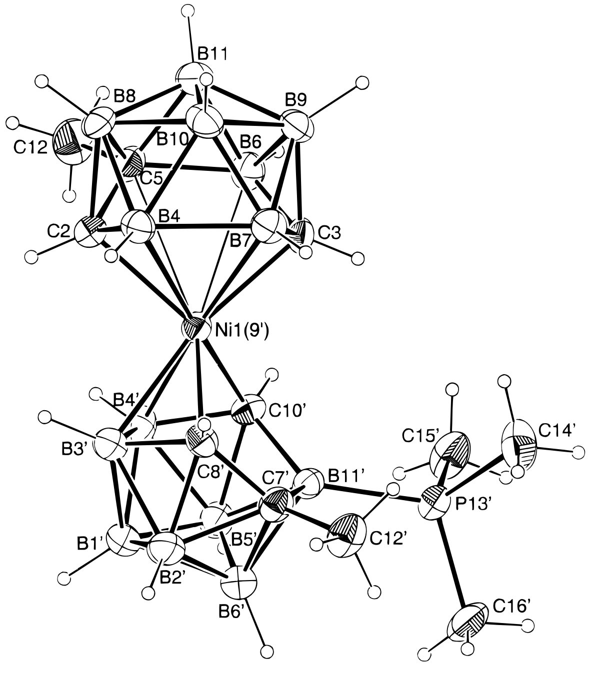

Figure 9. ORTEP drawing of the molecular structure of **5**, *commo-Ni*-(1-Ni-5-Me-2,3,5-$C_3B_7H_9$)(9′-Ni-7′-Me-11′-PMe_3-7′,8′,10′-$C_3B_7H_8$).

NMR spectra also show, as expected for a complex containing only one type of enantiomeric cage, only one methyl and two C−H resonances. Therefore, the spectra of **4a** strongly indicate that it has the *R*−*M*−*R*/*S*−*M*−*S* structure observed for **1a** and **3a**.

Reactions of $(MeC_3B_7H_9)_2M$ Complexes with Phosphines. The $(MeC_3B_7H_9)_2Pt$ complexes were found to be unreactive toward trimethylphosphine, but $(MeC_3B_7H_9)_2Ni$ was found to readily react (eq 6) to give a single product, **5**, in ~10% yield.

$$(MeC_3B_7H_9)_2Pt\ (\mathbf{3a{-}b}) + PMe_3 \rightarrow \text{no reaction} \qquad (5)$$

$$\begin{gathered}(MeC_3B_7H_9)_2Ni\ (\mathbf{4}) + PMe_3 \rightarrow \\ \textit{commo-Ni}\text{-}(1\text{-}Ni\text{-}5\text{-}Me\text{-}2,3,5\text{-}C_3B_7H_9) \\ (9'\text{-}Ni\text{-}7'\text{-}Me\text{-}11'\text{-}PMe_3\text{-}7',8',10'\text{-}C_3B_7H_8)\ (\mathbf{5})\end{gathered} \qquad (6)$$

The composition of **5** was established by both elemental analysis and exact mass determinations. The compound was determined to be paramagnetic, and the experimentally determined magnetic moment using the Evans method[5] is consistent with a single unpaired electron. The paramagnetism of **5** precluded characterization by NMR techniques, but a single-crystal X-ray determination established the *commo-Ni*-(1-Ni-5-Me-2,3,5-$C_3B_7H_9$)(9′-Ni-7′-Me-11′-PMe_3-7′,8′,10′-$C_3B_7H_8$) (**5**) structure shown in the ORTEP drawing given in Figure 9.

As can be seen in the diagram, rather than being bonded to the nickel atom, the trimethylphosphine is attached to the B11′ boron of one tricarbadecaboranyl cage. As a result, the two tricarbadecaboranyl cages have very different geometric structures and exhibit different metal coordination modes. It should also be noted that, in both cages of **5**, skeletal rearrangements have occurred so that the methyl groups are attached at the C5 and C7′ positions rather than at their original C2 and C8′ carbons, respectively. These migrations are similar to that found for one cage in **2** and were discussed earlier.

In Table 8, the nickel−tricarbadecaboranyl bond distances for the two NiC_3B_7 cage fragments in **5** are compared to those of two nickelatricarbadecaboranyl complexes having 11-vertex closo- and nido-type structures: *closo*-1-(η^3-C_3H_5)Ni(η^6-2-Me-2,3,5-$C_3B_7H_9$) and *nido*-9-(η^5-C_5H_5)Ni(η^4-8-Me-7,8,10-$C_3B_7H_9$).[2d] In **5**, the distances between the nickel atom and the four atoms of the unsubstituted cage, C2, B4, B7, and C3, are quite similar to those of the analogous four atoms of the PMe_3-substituted cage, C8′, B3′, B4′, and C10′, and both sets are typical of comparable distances in both *closo*-1-(η^3-C_3H_5)Ni(η^6-2-Me-2,3,5-$C_3B_7H_9$) and *nido*-9-(η^5-C_5H_5)Ni-(η^4-8-Me-7,8,10-$C_3B_7H_9$) (**6**). The nickel atom to C7′ (2.925(5) Å) and B11′ (2.878(6) Å) distances in the PMe_3-substituted cage are similar to those observed for *nido*-9-(η^5-C_5H_5)Ni(η^4-8-Me-7,8,10-$C_3B_7H_9$) and are consistent with those expected for an 11-vertex nido cage fragment. However, the distances from the nickel atom to C5 (2.709(5) Å) and B6 (2.633(6) Å) in the unsubstituted cage are much shorter and fall between those of the corresponding distances in the *closo*-1-(η^3-C_3H_5)Ni(η^6-2-Me-2,3,5-$C_3B_7H_9$) (Ni−C5, 2.515(3) Å; Ni−B6, 2.397(3) Å) and *nido*-9-(η^5-C_5H_5)Ni(η^4-8-Me-7,8,10-$C_3B_7H_9$) (Ni−C7, 2.880(5) Å; Ni−B11, 2.871(7) Å) complexes. Thus, in the unsubstituted tricarbadecaboranyl cage, the NiC_3B_7 appears to have a distorted geometry intermediate between those expected for 11-vertex closo (24 skeletal electrons) and nido (26 skeletal electrons) geometries and is similar to that of the structure exhibited by the CoC_3B_7 fragments in the 19-electron complexes 1-(η^5-C_5H_5)Co-2-Me-2,3,5-$C_3B_7H_9$[2d] (**7**) and *commo-Co*-(1-Co-2-Me-2,3,5-$C_3B_7H_9$)$_2$.[2b] This suggests that the cage distortion observed in the unsubstituted cage in **5** arises, as proposed in the cobalt complexes, because of localization of the extra unpaired electron in a cage, rather than a metal-centered, orbital thus giving a cage with an intermediate nido/closo electron count and cage structure.

Discussion

Studies of ferratricarbadecaboranyl complexes such as 1-(η^5-C_5H_5)Fe-2-Me-2,3,5-$C_3B_7H_9$ and *commo-Fe*-(1-Fe-2-Me-2,3,5-$C_3B_7H_9$)$_2$ have demonstrated that the *nido*-6-Me-5,6,9-$C_3B_7H_9$ ligand can form sandwich complexes in which the tricarbadecaboranyl cage can function as a 5-electron donor, analogous to the cyclopentadienyl group.[2] As described herein, the *nido*-6-Me-5,6,9-$C_3B_7H_9^-$ anion was also found to react with platinum group metal dihalides to give a new series of sandwich complexes of the formula (η^4-$MeC_3B_7H_9$)$_2$M. Each of these neutral (η^4-$MeC_3B_7H_9$)$_2$M complexes exhibits open 11-vertex cage geometries with the metal atoms occupying four-coordinate cage positions and

---

(12) For examples, see: (a) Mingos, D. M. P.; Forsyth, M. I.; Welch, A. J. *J. Chem. Soc., Dalton Trans.* **1978**, 1363−1374. (b) Barker, G. K.; Green, M.; Spencer, J. L.; Stone, F. G. A.; Taylor, B. F.; Welch, A. J. *J. Chem. Soc., Chem. Commun.* **1975**, 804−805. (c) Boocock, S. K.; Greenwood, N. N.; Hails, M. J.; Kennedy, J. D.; McDonald, W. S. *J. Chem. Soc., Dalton Trans.* **1981**, 1415−1429. (d) Beckett, M. A.; Greenwood, N. N.; Kennedy, J. D.; Thornton-Pett, M. *Polyhedron* **1985**, *4*, 4505−4511. (e) Cheek, Y. M.; Greenwood, N. N.; Kennedy, J. D.; McDonald, W. S. *J. Chem. Soc., Chem. Commun.* **1982**, 80−81. (f) Green, M.; Spencer, J. L.; Stone, F. G. A.; Welch, A. J. *J. Chem. Soc., Chem. Commun.* **1974**, 571−572. (g) Carr, N.; Mullica, D. F.; Sappenfield, E. L.; Stone, F. G. A. *Inorg. Chem.* **1994**, *33*, 1666−1673. (h) Kennedy, J. D. *Prog. Inorg. Chem.* **1986**, *34*, 211−434.

(13) (a) Klanberg, F.; Wegner, P. A.; Parshall, G. W.; Muetteries, E. L. *Inorg. Chem.* **1968**, *7*, 2072−2077. (b) Guggenberger, L. J. *J. Am. Chem. Soc.* **1972**, *94*, 114−119.

these structures are analogous to those that have been observed for the isoelectronic anionic metallaborane[13] complexes $(B_{10}H_{12})_2M^{2-}$ (M = Ni, Pd, Pt) that are derived from the formal $B_{10}H_{12}{}^{2-}$ anion.

If the tricarbadecaboranyl cages in these complexes are functioning as 5-electron donors, then the metals would have 20 valence electrons. While the corresponding Cp_2Pt and Cp_2Pd complexes have not been isolated, nickelocene, Cp_2Ni, has been shown to be a paramagnetic 20 valence electron complex with two unpaired electrons.[14] However, the $(\eta^4\text{-MeC}_3B_7H_9)_2M$ complexes **1**−**4**, like the isoelectronic $(B_{10}H_{12})_2M^{2-}$ complexes,[12] were found to be diamagnetic, and as discussed below, their observed open cage structures suggest that the metals are using only four metal orbitals in bonding to the two cages. Thus, these complexes should be viewed as 16-electron complexes, with the *nido*-6-Me-5,6,9-$C_3B_7H_9$ cage functioning as only a bidentate, 3-electron ligand similar to an $\eta^3\text{-}C_3H_5$ group. The complexes can then be considered as analogs of the well-known 16-electron bis(allyl) complexes, $(\eta^3\text{-}C_3H_5)_2M$ (M = Ni, Pd, Pt).[3]

From a cluster point of view, a platinum group $MeC_3B_7H_9M$ fragment, like a $(\eta^3\text{-}C_3H_5)M$ group, would be capable of donating one skeletal electron to another tricarbadecaboranyl cage. Therefore, on the basis of simple electron-counting rules,[15] an 11-vertex $MeC_3B_7H_9M$ (M = Ni, Pd, Pt) cage would, like in the $(MeC_3B_7H_9)_2Fe$ complexes, have 24 skeletal electrons, and thus should adopt a closo-octadecahedral geometry with the metal atoms in the six-coordinate cage positions. This prediction assumes both that the metal atom obeys the 18-electron rule and that the metal donates three orbitals for cage bonding. In the observed structures, the metal atoms occupy only four-coordinate cage positions, and as a result, open cage structures are generated that are similar in appearance to those that have been observed for 11-vertex 26 skeletal electron clusters. Given, as discussed above, that the metals do not have 20 valence electron configurations, then these open structures most likely arise, not from an increase in the cage electron count but rather from a decrease in the orbital contribution of the metal fragment so that the tricarbadecaboranyl fragment is functioning as only a bidentate ligand. Similar bonding patterns are observed in dicarbaborane and borane clusters containing platinum and palladium.[12,16] For example, the metalla(II)bis(dicarbollide) anionic complexes, $(1,2\text{-}C_2B_9H_{11})_2M^{2-}$, M = Pd, Pt, exhibit “slipped” sandwich configurations where the metal is shifted closer to the boron atoms and away from the carbon atoms on the two dicarbollide bonding faces[16] and, indeed, both Hawthorne[16a−c] and Wing[16d,e] have described these types of slipped complexes as analogs of π-allylic metal complexes.

The diamagnetic properties and metal η^4-coordination mode exhibited by $(\eta^4\text{-MeC}_3B_7H_9)_2Ni$ (**4**) and $(B_{10}H_{12})_2Ni^{2-}$ [13] (as well as by the NiC_3B_7 cage fragment in the triple-decker complex $(\eta^5\text{-}C_5H_5)Co(\mu\text{-}\eta^4\text{-MeEt}_4C_3B_2)Ni(\eta^4\text{-8-Me-7,8,10-}C_3B_7H_9)$[2d]) contrast sharply with the paramagnetism observed for the related tricarbahexaboranyl nickel complexes[17a] $(\eta^5\text{-2,3,5-}R_6C_3B_3)Ni(\eta^5\text{-1,3-}R_5C_3B_2)$[17] and $(\eta^5\text{-2,3,5-}R_6C_3B_3)_2Ni$[17,18] and the bis(1,7-dicarbollide)nickel(II) anionic complex $(1,7\text{-}C_2B_9H_{11})_2Ni^{2-}$.[16,19] The nickel(II) ions in these complexes apparently have, like nickelocene, 20-electron configurations with two unpaired electrons. Also, in spite of their higher electron counts, their structures are not significantly slipped but show near closo metallacarborane cage geometries. Thus, in these Ni(II) complexes the η^5, 5-electron bonding mode to the five-membered faces of the tricarbahexaboranyl and dicarbollide ligands is strongly favored, regardless of the 20-electron count. On the other hand, in **4** the nickel can more readily slip to one side of the puckered six-membered open face of the 10-vertex tricarbadecaboranyl ligand in order to reduce both its coordination from η^6 to η^4 and the ligand electron donation to the metal from 5 to 3 and thereby avoid the high-energy 20 valence electron configuration.

The similarity of the $(\eta^4\text{-MeC}_3B_7H_9)_2M$ complexes to the $(\eta^3\text{-}C_3H_5)_2M$ (M = Ni, Pd, Pt) complexes suggested that they might, like the $(\eta^3\text{-}C_3H_5)_2M$ complexes, undergo addition reactions with suitable bases. For example, the 16-electron $Ni(\eta^3\text{-}C_3H_5)_2$ complex is known to react (eq 7) with phosphines to initially form 18-electron adducts,[20] which then undergo ligand slippage at higher temperatures. On the other hand, the Pt(II) and Pd(II) η^3-allyl complexes react (eq 8) with phosphines to give 16-electron complexes where one allyl rearranges from η^3 to η^1.

$$(\eta^3\text{-}C_3H_5)_2Ni + PMe_3 \rightarrow (\eta^3\text{-}C_3H_5)_2Ni\cdot PMe_3 \quad (7)$$

$$(\eta^3\text{-}C_3H_5)_2M + PMe_3 \rightarrow (\eta^1\text{-}C_3H_5)M(\eta^3\text{-}C_3H_5)\cdot PMe_3 \qquad M = Pd,\ Pt \quad (8)$$

No reaction of the $(\eta^4\text{-MeC}_3B_7H_9)_2Pt$ complex with PMe_3 was observed, but since there is no easy rearrangement that would allow for further ring slippage of the tricarbadecaboranyl from the η^4-coordination to an η^2- or η^1-geometry, this is not unexpected. The $(\eta^4\text{-MeC}_3B_7H_9)_2Ni$ complex (**4**), however, readily reacted, but the expected metal-coordinated phosphine adduct-complex, $(MeC_3B_7H_9)_2Ni\cdot PMe_3$, was not observed. Instead, the 17 valence electron compound **5**, where the phosphine is attached to one boron atom on the cage rather than to the Ni, was isolated. A similar phosphine migration from a nickel atom to a cage boron site in another nickelacarborane had been previously observed by Hawthorne in the thermal rearrangement of *closo*-3-$(PPh_3)_2Ni$-1,2-$C_2B_9H_{11}$ to *closo*-3-$(PPh_3)(H)Ni$-8-PPh_3-

---

[14] (a) Fritz, H. P.; Schwarzhans, K.-E. *J. Organomet. Chem.* **1963**−**1964**, *1*, 208−211. (b) Prins, P.; van Voorst, J. D. W.; Schinkel, C. J. *Chem. Phys. Lett.* **1967**, *1*, 54−55.

[15] (a) Williams, R. E. *Inorg. Chem.* **1971**, *10*, 210−214. (b) Wade, K. *Adv. Inorg. Chem. Radiochem.* **1976**, *18*, 1−66. (c) Williams, R. E. *Adv. Inorg. Chem. Radiochem.* **1976**, *18*, 67−142. (d) Rudolph, R. W. *Acc. Chem. Res.* **1976**, *9*, 446−452. (e) Williams, R. E. In *Electron Deficient Boron and Carbon Clusters*; Olah, G. A., Wade, K., Williams, R. E., Eds.; Wiley: New York, 1991; pp 11−93. (f) Williams, R. E. *Chem. Rev.* **1992**, *92*, 177−207.

[16] (a) Hawthorne, M. F.; Young, D. C.; Andrew, T. D.; Howe, D. V.; Pilling, R. L.; Pitts, A. D.; Reintjes, M.; Warren, L. F.; Wegner, P. A. *J. Am. Chem. Soc.* **1968**, *90*, 879−896. (b) Hawthorne, M. F.; Dunks, G. B. *Science* **1972**, *178*, 7114. (c) Hawthorne, M. F.; Warren, L. F. *J. Am. Chem. Soc.* **1968**, *90*, 4823−4828. (d) Wing, R. M. *J. Am. Chem. Soc.* **1967**, *89*, 5599−5604. (e) Wing, R. M. *J. Am. Chem. Soc.* **1968**, *90*, 4828−4834.

[17] (a) Siebert, W. *Angew. Chem., Int. Ed. Engl.* **1985**, *24*, 943−958. (b) Kuhlmann, T.; Pritzkow, H.; Zenneck, U.; Siebert, W. *Angew. Chem., Int. Ed. Engl.* **1984**, *12*, 965−966. (c) Zwecker, J.; Kuhlmann, T.; Pritzkow, H.; Siebert, W.; Zenneck, U. *Organometallics* **1988**, *7*, 2316−2324.

[18] Zwecker, J.; Pritzkow, H.; Zenneck, U.; Siebert, W. *Angew. Chem., Int. Ed. Engl.* **1986**, *25*, 1099−1100.

[19] Wing, R. M. *J. Am. Chem. Soc.* **1970**, *92*, 1187−1190.

[20] Henc, B.; Jolly, P. W.; Salz, R.; Stobbe, S.; Wilke, G.; Benn, R.; Mynott, R.; Seevogel, K.; Goddard, R.; Krüger, C. *J. Organomet. Chem.* **1980**, *191*, 449−475.

1,2-$C_2B_9H_{10}$.[21] As depicted in Figure 10, it is possible that a similar type of rearrangement may occur for **5** involving the initial formation of the expected 18 valence electron bis(tricarbadecaboranyl)nickel•phosphine adduct, followed by a PMe_3−hydride exchange between the metal and cage. Oxidation and loss of a proton during the workup could then lead to the final product, **5**.

In conclusion, the above results have shown that the (η^4-$MeC_3B_7H_9)_2M$ (M = Ni, Pd, Pt) complexes **1**−**4** have structural and spectroscopic properties suggesting that the tricarbadecaboranyl ligands are functioning as only 3-electron donors to these metals. Thus, the complexes can be considered as the first *neutral* metallacarborane analogs of the platinum group π-allylic complexes (η^3-$C_3H_5)_2M$. However, an important difference between the tricarbadecaboranyl and π-allylic complexes is that since **1**−**4** do not undergo the metal elimination, ligand-coupling reactions characteristic of the organometallic compounds,[3] they are thermally stable at room temperature.

Most importantly, the above conclusions combined with the results of earlier metal coordination studies[2] also demonstrate that the tricarbadecaboranyl ligand can, depending upon the electronic and structural requirements of the metal atom, readily change both its electron donation from five to three electrons and its coordination mode from η^6 to η^4. These observations, coupled with the structural changes observed upon formation of **5**, further suggest that in certain complexes the tricarbadecaboranyl ligand might easily undergo *reversible* $\eta^6 \rightarrow \eta^4$ coordination, similar to the $\eta^5 \rightarrow \eta^3$ ring-slippage process proposed for some associative substitution reactions of cyclopentadienyl−metal[22] and dicarbollide−metal complexes.[23] Such facile rearrangements may then provide reversible low-energy pathways to open new coordination sites at the metal atoms in the tricarbadecaboranyl complexes.

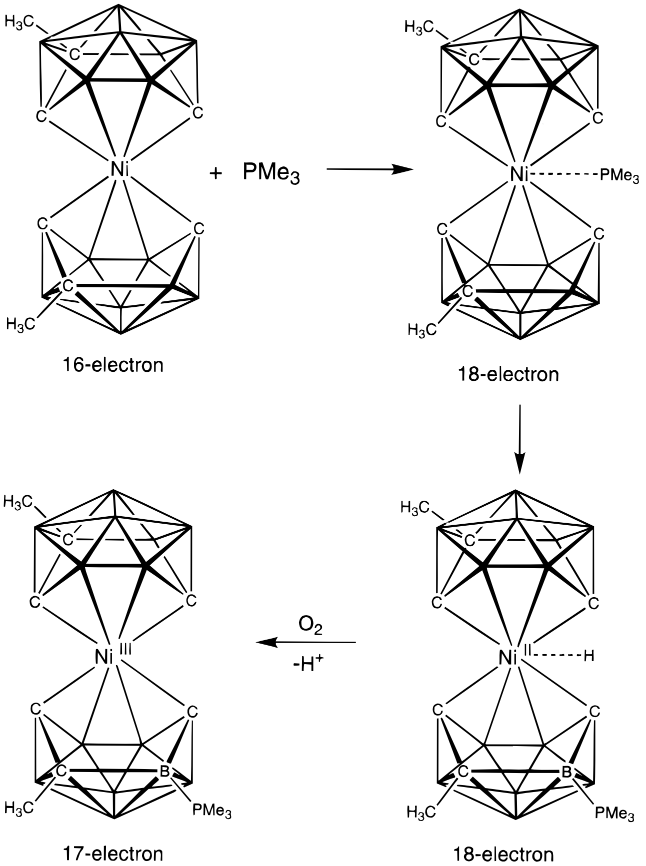

Figure 10. Possible reaction sequence leading to **5**, *commo-Ni*-(8-Ni-10-Me-7,9,10-$C_3B_7H_9$)(8′-Ni-10′-Me-11′-PMe_3-7′,9′,10′-$C_3B_7H_8$).

Acknowledgment. We thank the National Science Foundation for support of this work.

Supporting Information Available: Tables listing atomic coordinates, bond distances and angles, least-squares planes, and thermal parameters for **1a**, **2**, **3a**, **3b**, and **5** (57 pages). Ordering information is given on any current masthead page.

OM950762G

---

[21] Miller, S. B.; Hawthorne, M. F. *J. Chem. Soc., Chem. Commun.* **1976**, 786−787.

[22] Basolo, F. *New J. Chem.* **1994**, *18*, 19−24.

[23] Shen, J. K.; Zhang, S.; Basolo, F.; Johnson, S. E.; Hawthorne, M. F. *Inorg. Chim. Acta* **1995**, *235*, 89−97.